

Article

Flight Conflict Detection Algorithm Based on Relevance Vector Machine

Senlin Wang ^{1,2}  and Dangmin Nie ^{1,2,*}¹ Air Traffic Control and Navigation School, Air Force Engineering University, Xi'an 710051, China² National Key Laboratory, Air Traffic Collision Prevention, Xi'an 710051, China

* Correspondence: ndm863@163.com

Abstract: In response to the problems of slow running speed and high error rates of traditional flight conflict detection algorithms, in this paper, we propose a conflict detection algorithm based on the use of a relevance vector machine. A set of symmetrical historical flight data was used as the training set of the model, and we used the SMOTE resampling method to optimize the training set. We obtained relatively symmetrical training data and trained it with the relevance vector machine, improving the kernels through an intelligent algorithm. We tested this method with new symmetrical flight data. The improved algorithm greatly improved the running speed and was able to effectively reduce the missed alarm rate of in-flight conflict detection symmetrically, thus effectively ensuring flight safety.

Keywords: flight conflict detection; relevance vector machine; Bayesian optimization



Citation: Wang, S.; Nie, D. Flight Conflict Detection Algorithm Based on Relevance Vector Machine. *Symmetry* **2022**, *14*, 1992. <https://doi.org/10.3390/sym14101992>

Academic Editor: Theodore E. Simos

Received: 23 August 2022

Accepted: 19 September 2022

Published: 23 September 2022

Publisher's Note: MDPI stays neutral with regard to jurisdictional claims in published maps and institutional affiliations.



Copyright: © 2022 by the authors. Licensee MDPI, Basel, Switzerland. This article is an open access article distributed under the terms and conditions of the Creative Commons Attribution (CC BY) license (<https://creativecommons.org/licenses/by/4.0/>).

1. Introduction

With the rapid development of civil aviation and the rapid growth in flight volumes, ensuring flight safety has become an essential guarantee in the rapid development of the aviation industry. Flight conflict detection is a crucial method to ensure flight safety. According to aircraft tracking information, flight intention information and external environmental information provided by navigation equipment are used to identify flight conflicts between two aircrafts during the conflict detection time. Two methods are mainly used to solve the problem of flight conflict detection: the geometric method and the probability method [1]. The geometric conflict detection method is based on the use of geometric calculations to judge whether the aircraft has potential flight conflicts within the geometric range of the encounter. However, the problem with this method is that the actual situation cannot be represented by a strict geometric relationship between the aircrafts, and many factors need to be considered, such as the influence of wind, pilot operation, and the external environment.

As a result, the geometric conflict detection method suffers from issues including low certainty and large error values [2]. The study of probability approaches with some fault tolerance is growing in popularity due to the numerous issues with geometric methods that are caused by the mistakes in flight data. Traditional probabilistic conflict detection methods include those based on probability flow theory, complex networks, Markov chains, game theory, and other methods [3–5]. In 2000, Prandini and others used the probability analysis method to analyze the measurement index of complex flight trade-offs and established a flight collision avoidance model. Almost all subsequent studies have improved and expanded upon this model [6]. Shi Lei and others proposed a probabilistic short-term conflict detection algorithm based on the idea of a hybrid system and position space discretization, which uses the tracking and intention information in relation to monitoring information to predict the short-term track of a flight based on the state-related random linear hybrid system [7]. Daalen et al. used probability flow theory to solve the upper probability bound of overall flight conflicts. Jacquemart et al. proposed the simulation of aircraft motion rollout with the use of a Markov chain, and used an important

sampling method to calculate conflict probabilities [8]. Compared with the above methods, intelligent methods, such as support vector machines, have the advantages of strong real-time performance, high accuracy, relatively small calculation, and small error values, so they have become a new hot spot in flight conflict detection research [9,10].

In the research on the solution of conflict detection problems through a support vector machine, Jiao Yuliang and others first used a support vector machine to propose the use of the horizontal two-dimensional conflict detection method for high-altitude routes [11]. Han Dong and others used the support vector machine method to detect flight conflicts based on an ellipsoidal protected area, and used simulation data to train the classifier in advance to carry out efficient conflict detection suitable for low-altitude flights [12]. Wu Minggong and others combined the support vector machine classification algorithm, the sigmoid function, and an elliptical protected area to establish a flight conflict detection model that can simultaneously output the conflict or lack thereof and its probability of occurrence [13]. On this basis, Wang Ershen used the improved ID3 decision tree algorithm to reduce the search space to a local method to screen the aircraft with potential flight conflicts, used the random forest method to select the appropriate training set, and used the tanh-function optimization to easily saturate the sigmoid function. A probability map of SVM classification obtains the following results [14]: the above methods have all been used to study flight conflict detection problems with the use of a support vector machine, but support vector machines have many disadvantages. For example, an SVM cannot calculate the posterior probability distribution of a sample output, an SVM is not suitable for multi-classification problems, and SVM hyperparameters need to be obtained through cross-validation, which is very time-consuming. Furthermore, the kernel of an SVM must be positive and definite, whereas RVM avoids these disadvantages. Compared to SVM, a relevance vector machine can better meet the mission needs of flight conflict detection. In this paper, we propose a flight conflict detection method based on the use of a relevance vector machine. Using the SMOTE resampling method to optimize the training set, we establish an ellipsoidal protected area model, analyze historical flight data, establish an RVM classification model, and optimize the kernel through various intelligent algorithms, as well as comprehensively analyzing and selecting the best kernels. In terms of the running speed, this method only takes 0.001 s to run, an extremely fast running speed. In terms of classification accuracy, the optimized relevance vector machine model exhibits a 20% higher accuracy than the SVM model. In terms of innovation, this study represents the first time an RVM has been employed in flight conflict detection. In applications, by loading the trained classifier before take-off, the flight conflict detection speed can be effectively improved, and flight safety can thus be guaranteed.

2. Methods

Flight conflict detection is a two-classification problem, with only two results: conflict or non-conflict. In previous studies, the excellent two-classification machine learning algorithm of the SVM (support vector machine) was used to solve flight conflict detection problems. Although SVM has good promotion ability and avoids the local optimum, there are still problems such as its slow speed on the testing set and its low classification accuracy. Compared with support vector machines, the algorithm used in this paper can give a probabilistic output and it has the following advantages: better generalization ability, better sparsity, more flexible kernel selection, no mandatory positive definite, and simpler parameter settings. Conflict detection requires a high running speed, and RVM has better sparsity than SVM, so its speed on testing sets is faster. Therefore, in this paper, we propose a flight conflict detection method based on the use of a relevance vector machine to solve this problem.

2.1. Data Preprocessing

We first obtain the current position information for the two aircrafts and the speed vectors through the ADS-B system. The position information of the two aircrafts is $X_a = (x_a, y_a, z_a)$, $X_b = (x_b, y_b, z_b)$, and the speed vectors of the two aircrafts are $V_a = (v_{xa}, v_{ya}, v_{za})$ and $V_b = (v_{xb}, v_{yb}, v_{zb})$. We extract the feature quantity, reduce the sample dimension, and obtain the sample information $X = X_a - X_b = (x, y, z)$, $V = V_a - V_b = (v_x, v_y, v_z)$ and use a detection time t , to obtain a simplified sample with a sample feature dimension of 7 [15–17], that is:

$$F = (x, y, z, v_x, v_y, v_z, t) \quad (1)$$

In airspace, the probability of free flight conflicts is a small event in regard to the total sample, so there is an overwhelming advantage for the collected samples without conflicts. In order to avoid this imbalance in the number of samples affecting the conflict detection process, the number of positive and negative samples should be roughly balanced. We improve the robustness of the model to the sample set through the a relatively symmetrical training set. We improve the classification ability through the SMOTE resampling method, that is, by inserting virtual samples between adjacent negative samples to reduce the occurrence of over-adaptation [18]. At the same time, normalization of the data is performed:

$$Y = \frac{X - X_{\min}}{X_{\max} - X_{\min}} \quad (2)$$

wherein $Y \in [0, 1]$ is the normalized value, X is the sample eigenvalue, and X_{\max} , and X_{\min} are the maximum and minimum eigenvalues in the total sample, respectively.

2.2. Definition of Relevance Vector Machine

The given training set is $G = \{(x_i, h_i)\}_{i=1}^N$, where $\{x_i\}_{i=1}^N$ is the input sample vector, $\{h_i\}_{i=1}^N$ represents the corresponding target value, and N is the total number of samples. The basic form of the relevance vector machine model output is [19–27]:

$$y(x, w) = \sum_{i=0}^N w_i K(x, x_i) + w = \varphi(x)w \quad (3)$$

Among them, w is the weight value vector, $K(x, x_i)$ is the kernel, and $\varphi(x)$ is the $M \times (M + 1)$ order kernel matrix. Assuming that m_i it obeys the normal distribution with a mean value of $y(x_i, w)$ and a variance of σ^2 , it is expressed by probability as

$$p(h_i) = N(h_i | y(x_i; w), \sigma^2) \quad (4)$$

The likelihood function of the sample is

$$p(h | w, \sigma^2) = \prod_{i=0}^N N(h_i | y(x_i; w), \sigma^2) = (2\pi\sigma^2)^{-\frac{N}{2}} \exp\left\{-\frac{\|h - \Phi w\|^2}{2\sigma^2}\right\} \quad (5)$$

The conditional probability is

$$P(h_* | h) = \int P(h_* | w, \sigma^2) p(w, \sigma^2 | h) dw d\sigma^2 = \int P(h_* | w, \sigma^2) \frac{p(h | w, \sigma^2) p(w, \sigma^2)}{p(h)} dw d\sigma^2 \quad (6)$$

In order to avoid overfitting, the relevance vector machine adds prerequisites to the weight vector w , so that w is a standard normal distribution, so there are:

$$p(w | \mu) = \prod_{i=0}^N N(w_i | 0, \mu_i^{-1}) = \prod_{i=0}^N \frac{\mu_i}{\sqrt{2\pi}} \exp\left\{-\frac{\mu_i w_i^2}{2}\right\} \quad (7)$$

In this case, the required conditional probability formula is

$$P(h_*|h) = \int P(h_*|w, \mu, \sigma^2) p(w, \mu, \sigma^2|h) dw d\mu d\sigma^2 \quad (8)$$

In the formula $\mu = [\mu_0, \mu_1, \mu_2, \dots, \mu_N]^T$ is a $N + 1$ -dimensional hyperparameter vector, which obeys the Gamma distribution. Through the Bayesian theory, we can find:

$$p(w, \mu, \sigma^2|h) = P(w|h, \mu, \sigma^2) p(\mu, \sigma^2|h) \quad (9)$$

In the formula:

$$p(w|h, \mu, \sigma^2) = \frac{p(h|w, \sigma^2) p(w|\mu)}{p(h|\mu, \sigma^2)} = (2\pi)^{-\frac{N+1}{2}} |\Phi|^{-\frac{1}{2}} \exp\left\{-\frac{(w-\alpha)^T \Sigma^{-1} (w-\alpha)}{2}\right\} \quad (10)$$

$$\Phi = (\sigma^2 \varphi^T \varphi + A)^{-1} \quad (11)$$

$$\alpha = \sigma^{-2} \Phi \varphi^T h \quad (12)$$

$$A = \text{diag}(\mu_0, \mu_1, \mu_2, \dots, \mu_N) \quad (13)$$

From the delta approximation function $P(\mu, \sigma^2|h) \approx \delta(\mu_{MP}, \sigma_{MP}^2)$, we can get:

$$P(h_*|h) \approx \int P(h_*|w, \mu_{MP}, \sigma_{MP}^2) P(w|h, \mu_{MP}, \sigma_{MP}^2|h) dw \quad (14)$$

Integrating the above formula yields:

$$p(h_*|h, \mu_{MP}, \sigma_{MP}^2) = N(h_*|y_*, \sigma_*^2) \quad (15)$$

$$y_* = \varphi(x_*) \alpha \quad (16)$$

$$\sigma_*^2 = \sigma_{MP}^2 + \varphi\left(\begin{smallmatrix} x \\ * \end{smallmatrix}\right)^T T \Phi \varphi(x_*) \quad (17)$$

The solution of the model can be further transformed into how to obtain μ_{MP} and σ_{MP}^2 , which can be obtained by using the maximum likelihood method:

$$P(h|w, \sigma^2) P(w, \mu) dw = 2\pi^{-\frac{N}{2}} |\Omega|^{-\frac{1}{2}} \exp\left(-\frac{1}{2} h^T \Omega^{-1} h\right) \quad (18)$$

where $\Omega = \sigma^2 I + \varphi A^{-1} \varphi^T$. In the above formula, the solution of a and b with zero partial derivatives can be obtained:

$$\begin{aligned} \mu_i^{new} &= \frac{\gamma_i}{\mu^2} \\ (\sigma^2)^{new} &= \frac{\|h - \Phi \mu\|^2}{N - \sum_{i=0}^N \gamma_i} \\ \gamma_i &= 1 - \alpha_i \sum_{i,j} \end{aligned} \quad (19)$$

Among them, in the process of parameter change, a part of μ tends to infinity, and its corresponding weight value vector w will tend to zero. This means that a part of the corresponding basis function is "eliminated", and when the final result converges, the w corresponding to the remaining μ is the relevance vector we need.

2.3. Flight Conflict Detection Model

Flight conflict detection involves detecting the aircraft within the scope of the airspace through the use of navigation equipment to determine whether the aircraft can continuously meet the requirements of the minimum safety interval within a certain period of time. If the minimum safety interval is not met at the time t , it is determined that there is a flight

conflict. The ellipsoid protected area is established with the aircraft as the center. The protected area can be formulated as follows [28]:

$$\frac{x - x_0}{a^2} + \frac{y - y_0}{b^2} + \frac{z - z_0}{c^2} \leq 1 \quad (20)$$

wherein a , b , and c represent x , y , and z , respectively, three half-axis focal lengths.

According to China's "Civil Aviation Air Traffic Management Rules [29]", $a = b = 1000$ m, and $c = 150$ m. These values are used to establish a protected area in Figure 1.

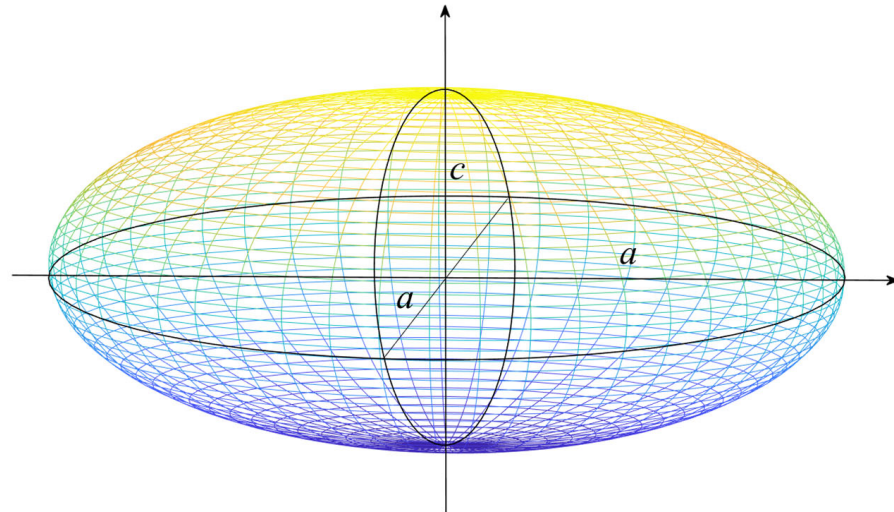


Figure 1. Protected area model.

3. Results

In this section, 10,000 sets of samples from the historical ADS-B dataset were first used as a training set for RVM training to analyze the feasibility of the proposed conflict detection method. The Gauss kernel with a strong nonlinearity mapping capability was selected as the kernel of the RVM, and 100 groups of samples were used to verify the accuracy of the conflict detection method. Secondly, the genetic algorithm, particle swarm algorithm, and Bayesian optimization were used to optimize the hyperparameters of the model. Finally, a comparison of the three optimization methods was carried out to prove the effectiveness of the relevance vector machine in flight conflict detection.

3.1. Accuracy Analysis of Conflict Detection Model

A simulation experiment was carried out on 100 pairs of dual-aircraft flight data in the training set, and the confusion matrix of the classification result and the result prediction diagram of the classification method were obtained. By comparing the predicted value and the actual conflict value, the accuracy of the method was analyzed.

Figure 2 shows a confusion matrix of the testing set without optimization. In the confusion matrix, TP in the upper left corner indicates that there was no conflict risk in real cases and there was no conflict in the prediction, while FP in the lower left corner indicates that there was a conflict risk in real cases, but there was no conflict in the prediction, and FN in the upper right corner indicates that there was no conflict risk in real cases, but there was a conflict in the prediction. Lastly, TN in the lower right corner indicates that there was a conflict risk in real cases and there was a conflict in the prediction. In the result prediction diagram (Figure 3), the blue line represents the actual conflict situation of the training set, and the red line represents the prediction result of the training set.

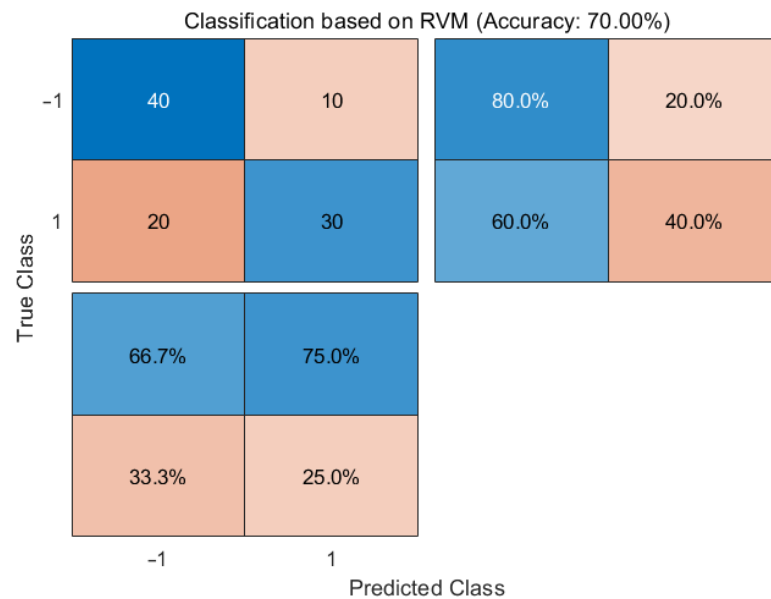


Figure 2. Confusion matrix of the relevance vector machine.

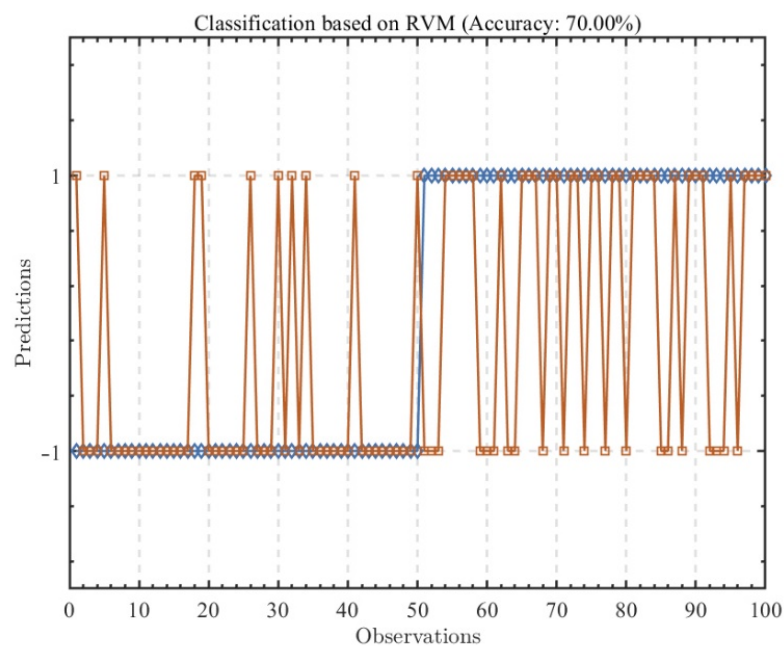


Figure 3. Prediction result graph of the relevance vector machine.

As can be seen in Figure 2, the training model without hyperparameter optimization still demonstrated a 70% accuracy. At the same time, judging from the ratio of TP and TN, after data preprocessing, the leakage missed alarm rate and false alarm rate of conflict risk maintained a relatively consistent level. The flight conflict detection method based on the RVM could be considered to have a certain feasibility, but it can also be seen that the accuracy of this method had great room for improvement. Thus, the detection accuracy of this method was improved through the optimization of the kernel.

3.2. Accuracy Analysis after Optimization of the Genetic Algorithm

In order to improve the accuracy in conflict detection and obtain a better RVM model, the kernel of the relevance vector machine was optimized by using a genetic algorithm [30].

As shown in Figures 4 and 5, in this case, the RVM training model optimized by means of a genetic algorithm displayed an 80% accuracy and was significantly improved before the phase angle optimization. At the same time, the missed alarm rate and false alarm rate of conflict risk maintained relatively consistent levels.

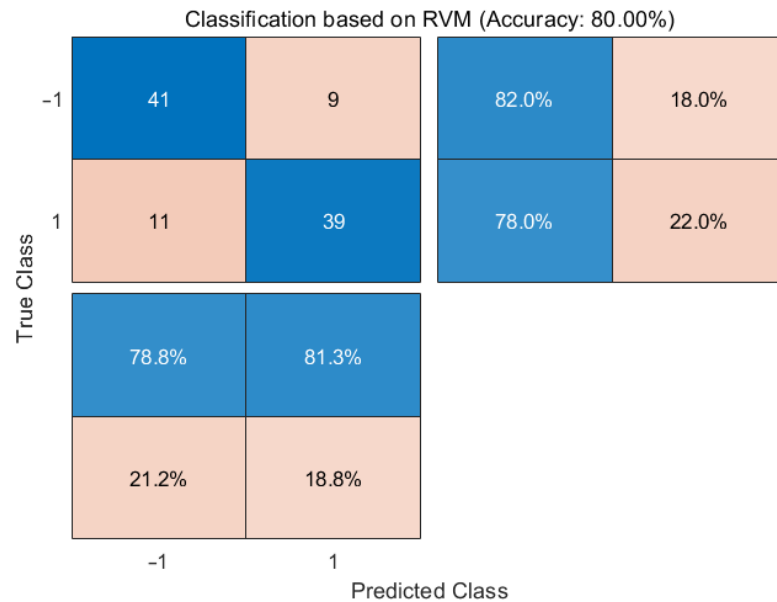


Figure 4. Confusion matrix after genetic algorithm optimization.

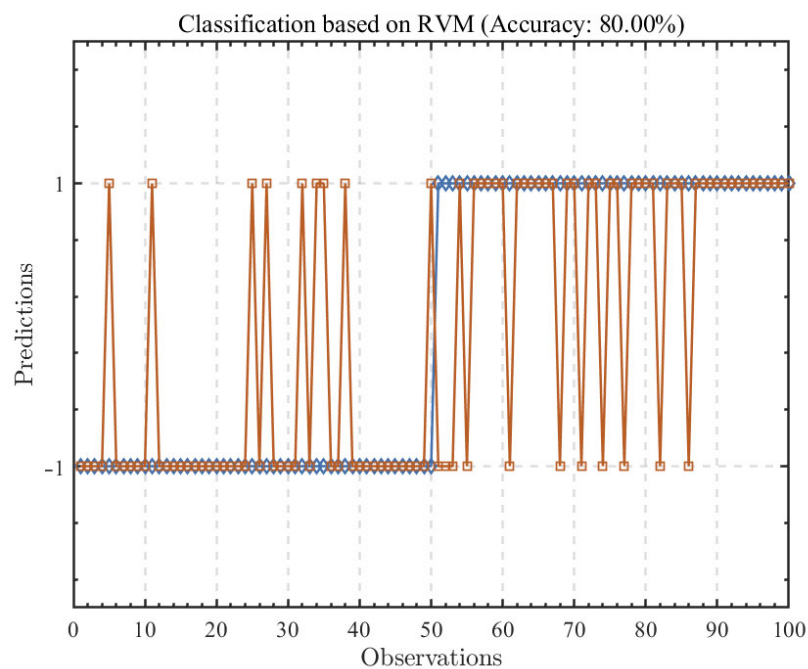


Figure 5. Improved genetic algorithm results prediction graph.

As shown in Figure 6, the optimization of the kernel was close to convergence after eight generations and had a good convergence rate. The disadvantage of this optimization approach is that the optimization speed cannot meet the requirements, and there is still room for improvement in its accuracy.

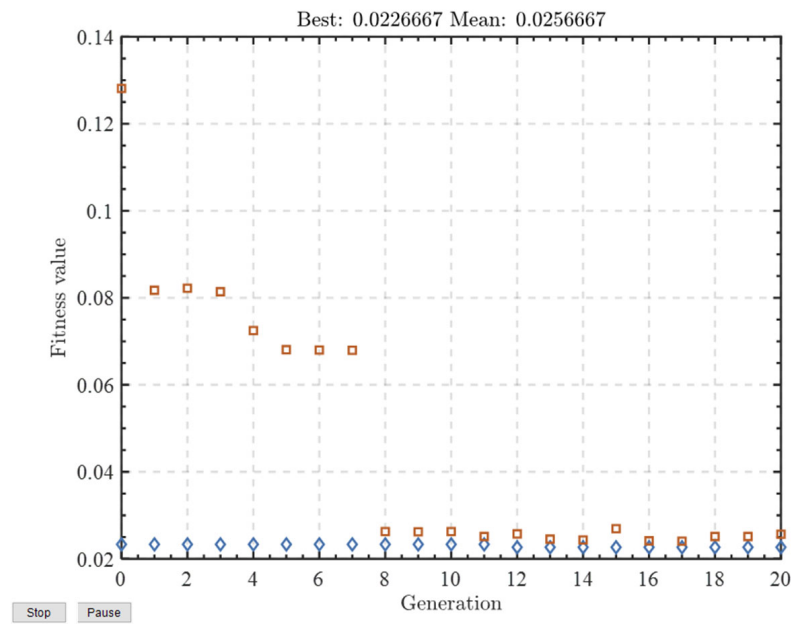


Figure 6. Genetic algorithm optimization process diagram.

3.3. Accuracy Analysis after Optimization of PSO Algorithm

The particle swarm optimization algorithm (PSO) is a swarm intelligence optimization algorithm that simulates the predation behavior of birds and fish. PSO has the advantages of a simple principle, a small amount of calculation, and fewer control parameters, so it is widely used in scheduling problems, optimization problems, path planning, and other practical problems. However, PSO still has some shortcomings, such as the fact that the algorithm easily falls into the local optimum, can easily become “precocious”, and has a slow convergence rate and low convergence accuracy [31–33]. As shown in Figures 7 and 8, the RVM kernel was optimized by means of particle swarm optimization, the optimized RVM model demonstrated an 81% accuracy in the classification of the training sets, and the optimized performance of the model was dramatically improved compared to the unoptimized model.

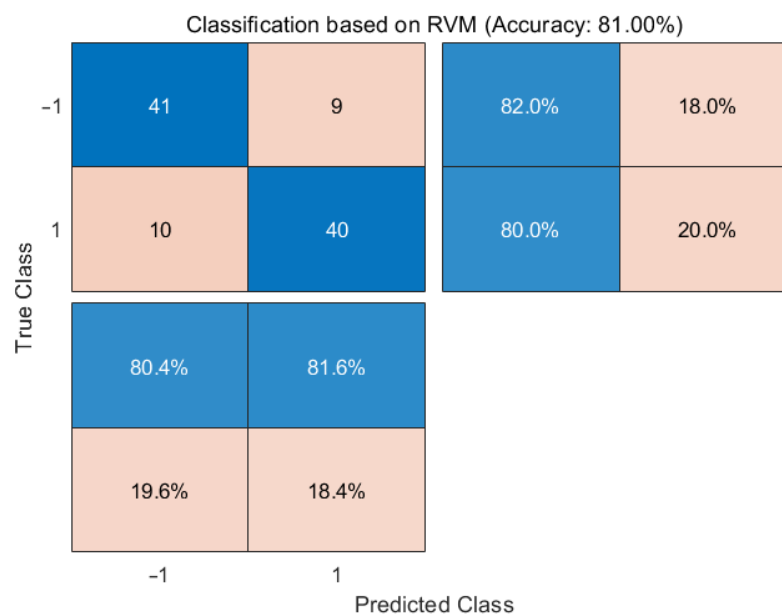


Figure 7. Confusion matrix after particle swarm optimization.

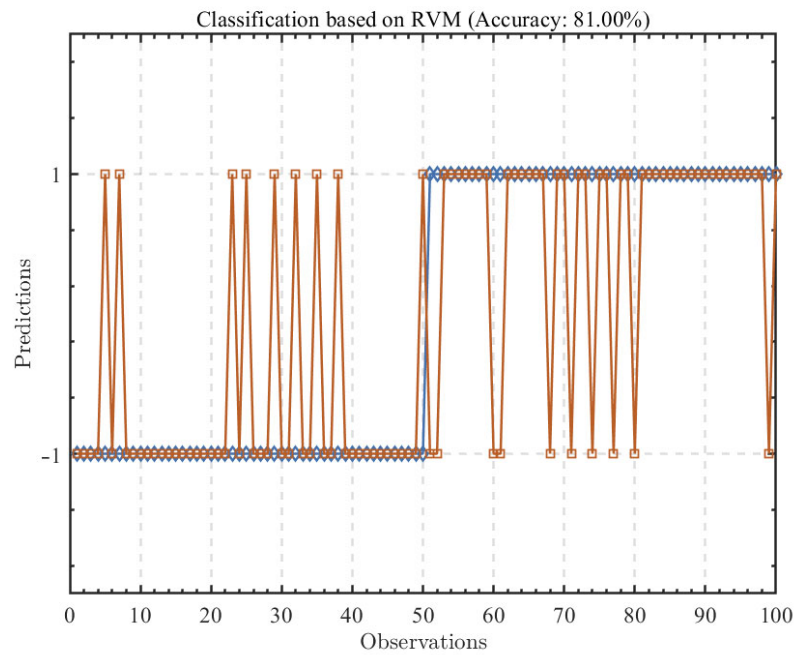


Figure 8. Results prediction chart based on improved particle swarm optimization.

3.4. Accuracy Analysis after Bayesian Optimization

Bayesian optimization (BO) is also called active optimization. This method is essentially model-based sequential optimization, and the next round can only be carried out after the end of the current round of evaluation. The subsequent evaluation position can be selected according to the information obtained by unknown objective functions to obtain the optimal solution at the least cost [34,35].

As shown in Figures 9 and 10, the model optimized by means of the Bayesian approach demonstrated the highest accuracy for the training set, and the balance between missed alarm rate and the false alarm rate was also the best of the four models, with extremely high symmetry for the classification results.

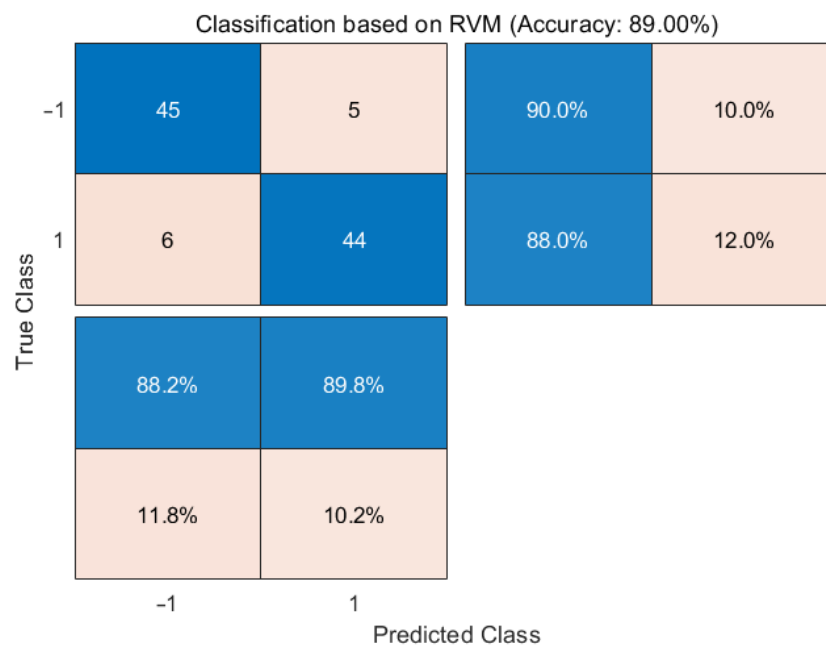


Figure 9. Confusion matrix after Bayesian optimization.

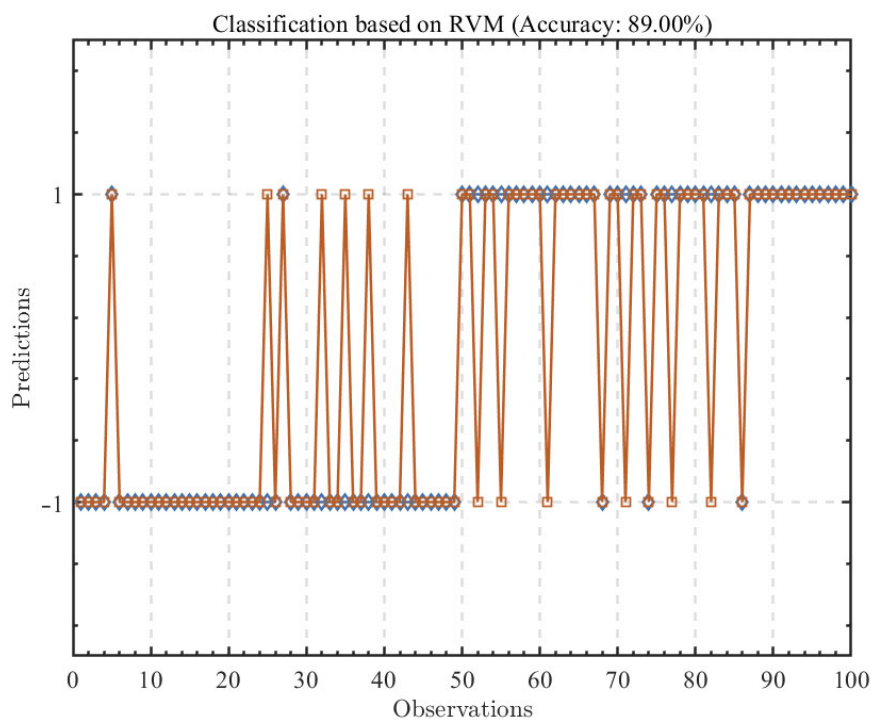


Figure 10. Results prediction chart based on Bayesian optimization.

As can be seen in Figures 11 and 12, in the process of Bayesian optimization, the fourth generation was already close to the optimal kernel, and the convergence rate was also the fastest of all the optimization methods.

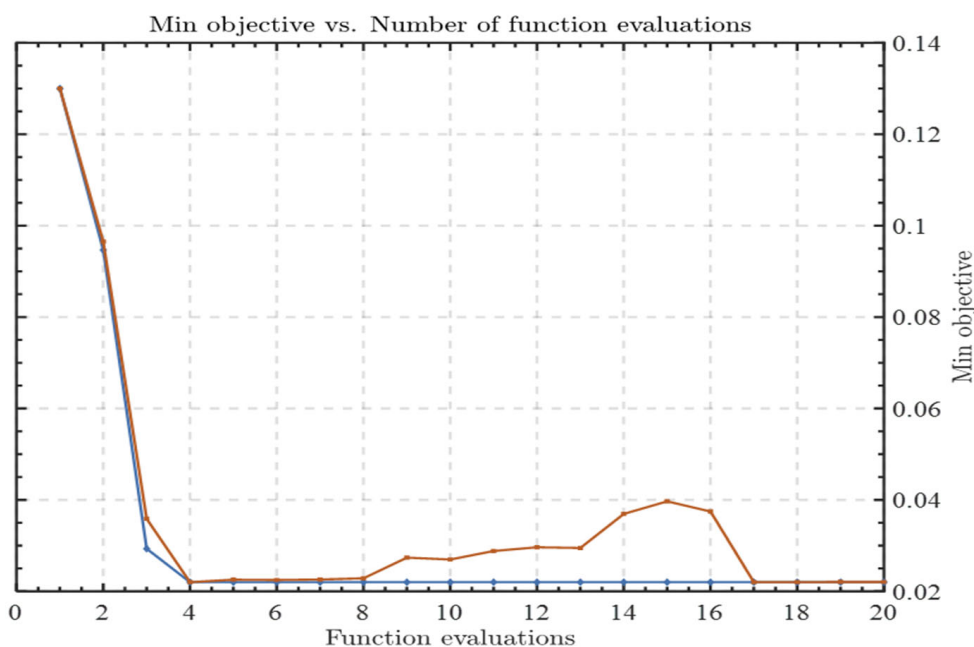


Figure 11. Bayesian optimization process diagram.

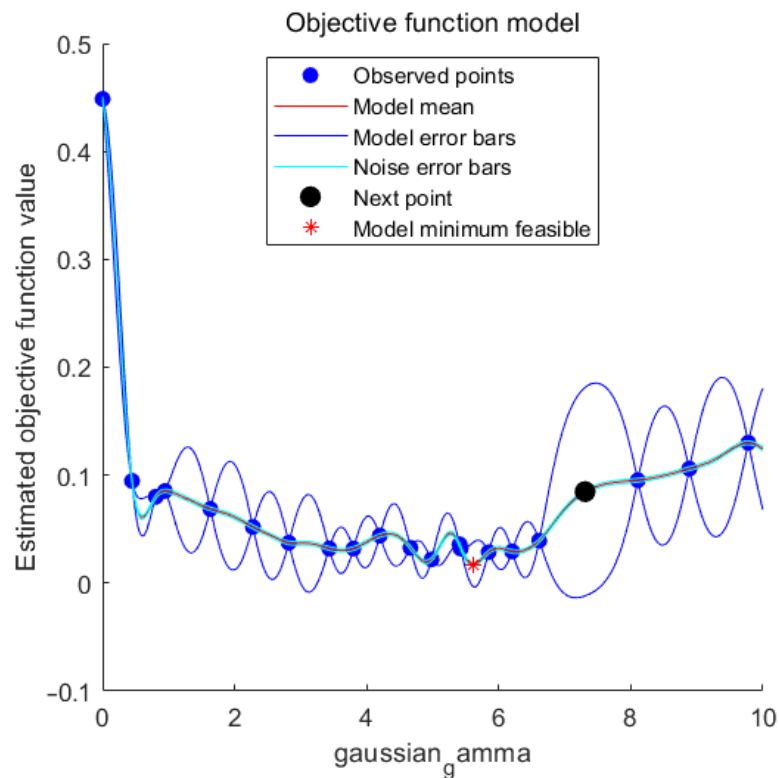


Figure 12. Variation diagram of Bayesian optimization function.

3.5. Optimization Effect Comparison

In order to verify the feasibility of this method for flight conflict detection and the optimized detection accuracy, the accuracy and running speed of the unoptimized flight conflict detection method based on the relevance vector machine were compared with those optimized using different methods in Table 1.

Table 1. Optimization effect comparison.

	SVM	RVM	GA-RVM	PSO-RVM	BO-RVM
Running speed	0.3 s	0.0048 s	0.0012 s	0.0019 s	0.0013 s
Optimization time			3418 s	3184 s	388 s
Accuracy	69%	70%	80%	81%	89%

Through this comparison, we observed that the flight conflict detection methods based on the use of the relevance vector machine were faster, and were thus able to meet the tight time demands of the urgent task of flight conflict detection. From the perspective of optimization speed, the Bayesian optimization method was much faster than the other two optimization methods. It is worth noting that, in fact, the three kinds of optimization refer to the optimization of the kernel. According to the different optimization effects, the obtained kernel was different, and its classification performance was also different. From the perspective of accuracy, Bayesian optimization demonstrated the best optimization effect, with a relatively balanced and low missed alarm and false alarm rates. Thus, it was able to meet the accuracy requirements of flight conflict detection during flight.

4. Conclusions

In this paper, we have proposed a flight conflict detection method based on the use of a relevance vector machine. The conflict risk in the flight process was judged by constructing a flight protection zone. The relevance vector machine was used to construct

the model, and the RVM model was trained with 10,000 data elements. The accuracy of the model was improved by optimizing the kernel. The model's performance was optimized by means of a genetic algorithm, a particle swarm algorithm, and a Bayesian optimization method. After optimization, the accuracy of flight conflict detection after Bayesian optimization was observed to be the highest, at 89%. At the same time, the results of this method exhibit a symmetrical missed alarm rate and false alarm rate. In addition, comparing the support vector machine and the relevance vector machine with the optimized kernel, the results show that the optimized conflict detection method based on the relevance vector machine displayed a better accuracy and a faster running speed, which verifies the effectiveness of the method. In practical applications, with its extremely fast running speed and high conflict detection accuracy, the flight conflict detection method based on RVM can reduce flight collision risks through its use as a pre-training model. It cannot be ignored that the flight conflict detection method based on the correlation vector machine still presents problems, such as a poor training ability for large samples and an accuracy which can still be improved. Our future work will focus on further improving the method's accuracy, and the influence of the hybrid kernel on the conflict detection effect will be discussed.

Author Contributions: Conceptualization, S.W.; methodology, S.W.; writing—original draft preparation, S.W.; writing—review and editing, S.W. and D.N.; visualization, D.N. All authors have read and agreed to the published version of the manuscript.

Funding: This research received no external funding.

Institutional Review Board Statement: Not applicable.

Informed Consent Statement: Not applicable.

Data Availability Statement: Not applicable.

Conflicts of Interest: The authors declare no conflict of interest.

References

1. Shi, L.; Wu, R.-B. Multi-route mid-term conflict detection algorithm based on discretization of predicted position space. *Signal Process.* **2012**, *28*, 1521–1528.
2. Goss, J.; Rajvanshi, R.; Subbarao, K. Aircraft conflict detection and resolution using mixed geometric and collision cone approaches. In Proceedings of the AIAA Guidance, Navigation, and Control Conference and Exhibit, Providence, RI, USA, 16–19 August 2004; p. 4879. [[CrossRef](#)]
3. Van Daalen, C.E.; Jones, T. Fast conflict detection using probability flow. *Automatica* **2009**, *45*, 1903–1909. [[CrossRef](#)]
4. Huang, Y.; Tang, J.; Lao, S. UAV flight conflict resolution algorithm based on complex network. *Acta Aeronaut. Astronaut. Sin.* **2018**, *39*, 262–274.
5. Zhang, X.; Guan, X.; Zhu, Y.; Lei, J. Strategic Flight Assignment Approach Based on Multi-Objective Parallel Evolution Algorithm with Dynamic Migration Interval. *Chin. J. Aeronaut.* **2015**, *28*, 556–563. [[CrossRef](#)]
6. Prandini, M.; Hu, J.; Lygeros, J.; Sastry, S. A probabilistic approach to aircraft conflict detection. *IEEE Trans. Intell. Transp. Syst.* **2000**, *1*, 199–220. [[CrossRef](#)]
7. Lei, S.; Ren-Biao, W.; Xiao-Xiao, H. Conflict Detection Algorithm Based on Overall Conflict Probability and Three Dimensional Brownian Motion. *J. Electron. Inf. Technol.* **2015**, *37*, 360–366.
8. Jacquemart, D.; Morio, J. Conflict probability estimation between aircraft with dynamic importance splitting. *Saf. Sci.* **2013**, *51*, 94–100. [[CrossRef](#)]
9. Liu, H.; Li, B.; Xiao, B.; Ran, D.; Zhang, C. Reinforcement learning-based tracking control for a quadrotor unmanned aerial vehicle under external disturbances. *Int. J. Robust Nonlinear Control* **2022**. [[CrossRef](#)]
10. Peral, J.; Gil, D.; Rotbei, S.; Amador, S.; Guerrero, M.; Moradi, H. A Machine Learning and Integration Based Architecture for Cognitive Disorder Detection Used for Early Autism Screening. *Electronics* **2020**, *9*, 516. [[CrossRef](#)]
11. Jiao, Y.L.; Zhang, X.J.; Guan, X.M. An Algorithm for Airborne Conflict Detection Based on Support Vector Machine. *Proc. Appl. Mech. Mater. Trans. Technol. Publ.* **2012**, *229*, 1140–1145.
12. Han, D.; Zhang, X.; Nie, Z.; Guan, X. A Conflict Detection Algorithm for Low-Altitude Flights Based on SVM. *J. Beijing Univ. Aeronaut. Astronaut.* **2018**, *44*, 576.
13. Jiang, X.; Wu, M.; Wen, X.; Wang, Z. Application of ensemble learning algorithm in aircraft probabilistic conflict detection of free flight. In Proceedings of the 2018 International Conference on Artificial Intelligence and Big Data (ICAIBD), Chengdu, China, 26–28 May 2018; pp. 10–14.

14. Wang, S.; Song, Y. Improved Model of Conflict Detection in Low Altitude Flight Based on SVM. *J. Beijing Univ. Aeronaut. Astronaut.* **2022**, *48*, 8–14. [[CrossRef](#)]
15. Zanin, M. Assessing Airport Landing Efficiency through Large-Scale Flight Data Analysis. *IEEE Access* **2020**, *8*, 170519–170528. [[CrossRef](#)]
16. Pan, Z.; Chi, C.; Zhang, J. A model of fuel consumption estimation and abnormality detection based on airplane flight data analysis. In Proceedings of the 2018 IEEE/AIAA 37th Digital Avionics Systems Conference (DASC), London, UK, 23–27 September 2018; pp. 1–6. [[CrossRef](#)]
17. Min, S. *A Proactive Safety Enhancement Methodology for General Aviation Using a Synthesis of Aircraft Performance Models and Flight Data Analysis*; Georgia Institute of Technology: Atlanta, GA, USA, 2018.
18. Jeatrakul, P.; Wong, K.W.; Fung, C.C. Classification of imbalanced data by combining the complementary neural network and SMOTE algorithm. In Proceedings of the International Conference on Neural Information Processing, Sydney, Australia, 22–25 November 2010; pp. 152–159. [[CrossRef](#)]
19. Yang, B.-S.; Gu, F.; Ball, A. Thermal Image Enhancement Using Bi-Dimensional Empirical Mode Decomposition in Combination with Relevance Vector Machine for Rotating Machinery Fault Diagnosis. *Mech. Syst. Signal Process.* **2013**, *38*, 601–614.
20. Jia, Y.; Kwong, S.; Wu, W.; Gao, W.; Wang, R. Generalized relevance vector machine. In Proceedings of the 2017 Intelligent Systems Conference (IntelliSys), London, UK, 7–8 September 2017; pp. 638–645.
21. Li, H.; Pan, D.; Chen, C.L.P. Intelligent Prognostics for Battery Health Monitoring Using the Mean Entropy and Relevance Vector Machine. *IEEE Trans. Syst. Man Cybern. Syst.* **2014**, *44*, 851–862. [[CrossRef](#)]
22. Mianji, F.A.; Zhang, Y. Robust Hyperspectral Classification Using Relevance Vector Machine. *IEEE Trans. Geosci. Remote Sens.* **2011**, *49*, 2100–2112. [[CrossRef](#)]
23. Deo, R.C.; Samui, P.; Kim, D. Estimation of monthly evaporative loss using relevance vector machine, extreme learning machine and multivariate adaptive regression spline models. *Stoch. Hydrol. Hydraul.* **2015**, *30*, 1769–1784. [[CrossRef](#)]
24. Demir, B.; Erturk, S. Hyperspectral Image Classification Using Relevance Vector Machines. *IEEE Geosci. Remote Sens. Lett.* **2007**, *4*, 586–590. [[CrossRef](#)]
25. Elarab, M.; Ticlavilca, A.M.; Torres-Rua, A.F.; Maslova, I.; McKee, M. Estimating chlorophyll with thermal and broadband multispectral high resolution imagery from an unmanned aerial system using relevance vector machines for precision agriculture. *Int. J. Appl. Earth Obs. Geoinf. ITC J.* **2015**, *43*, 32–42. [[CrossRef](#)]
26. Caesarendra, W.; Widodo, A.; Yang, B.-S. Application of relevance vector machine and logistic regression for machine degradation assessment. *Mech. Syst. Signal Process.* **2010**, *24*, 1161–1171. [[CrossRef](#)]
27. Widodo, A.; Kim, E.Y.; Son, J.-D.; Yang, B.-S.; Tan, A.C.; Gu, D.-S.; Choi, B.-K.; Mathew, J. Fault diagnosis of low speed bearing based on relevance vector machine and support vector machine. *Expert Syst. Appl.* **2009**, *36*, 7252–7261. [[CrossRef](#)]
28. Xu, Y.; Yu, G.; Wang, Y.; Wu, X.; Ma, Y. A Hybrid Vehicle Detection Method Based on Viola-Jones and HOG + SVM from UAV Images. *Sensors* **2016**, *16*, 1325. [[CrossRef](#)] [[PubMed](#)]
29. Civil Aviation Administration of China. *Rules for Air Traffic Management of Civil Aircraft: CCAR-93TM-R5*; Civil Aviation Administration of China: Beijing, China, 2017. (In Chinese)
30. Escamilla-Serna, N.J.; Seck-Tuoh-Mora, J.C.; Medina-Marin, J.; Barragan-Vite, I.; Corona-Armenta, J.R. A Hybrid Search Using Genetic Algorithms and Random-Restart Hill-Climbing for Flexible Job Shop Scheduling Instances with High Flexibility. *Appl. Sci.* **2022**, *12*, 8050. [[CrossRef](#)]
31. Li, Y.; Zhou, X.; Gu, J.; Guo, K.; Deng, W. A Novel K-Means Clustering Method for Locating Urban Hotspots Based on Hybrid Heuristic Initialization. *Appl. Sci.* **2022**, *12*, 8047. [[CrossRef](#)]
32. Ahmadian, A.; Elkamel, A.; Mazouz, A. An Improved Hybrid Particle Swarm Optimization and Tabu Search Algorithm for Expansion Planning of Large Dimension Electric Distribution Network. *Energies* **2019**, *12*, 3052. [[CrossRef](#)]
33. Garcia-Guarin, J.; Rodriguez, D.; Alvarez, D.; Rivera, S.; Cortes, C.; Guzman, A.; Bretas, A.; Aguero, J.R.; Bretas, N. Smart Microgrids Operation Considering a Variable Neighborhood Search: The Differential Evolutionary Particle Swarm Optimization Algorithm. *Energies* **2019**, *12*, 3149. [[CrossRef](#)]
34. Upreti, D.; Pignatti, S.; Pascucci, S.; Tolomio, M.; Huang, W.; Casa, R. Bayesian Calibration of the Aquacrop-OS Model for Durum Wheat by Assimilation of Canopy Cover Retrieved from VEN μ S Satellite Data. *Remote Sens.* **2020**, *12*, 2666. [[CrossRef](#)]
35. Otero-Casal, C.; Patlakas, P.; Prósper, M.A.; Galanis, G.; Miguez-Macho, G. Development of a High-Resolution Wind Forecast System Based on the WRF Model and a Hybrid Kalman-Bayesian Filter. *Energies* **2019**, *12*, 3050. [[CrossRef](#)]